JOURNAL OF MATERIALS SCIENCE 20 (1985) 85–96

The use of a δ-alumina fibre for metal–matrix composites

T. W. CLYNE, M. G. BADER, G. R. CAPPLEMAN, P. A. HUBERT
Department of Materials Science and Engineering, University of Surrey, Guildford, Surrey, UK

Composites formed by infiltration of an array of fine alumina fibres with aluminium alloy melts have been investigated in terms of fabrication characteristics, microstructural features and mechanical properties. A production method has been developed in which the application of pressure ensures very low porosity levels and strong fibre–matrix bonding. Details of the transport phenomena occurring during fabrication have been explored with a view to optimizing selection of applied pressure, thermal fields, alloy composition and the structure of the fibrous preform. Microstructural examinations revealed an intimate fibre–matrix bond, but the virtual absence of any chemical reaction at the interface. Comparison of property measurements with data from unreinforced alloys revealed increased elastic moduli and marked improvement in tensile strength at elevated temperature, accompanied by reductions in elongation.

1. Introduction

There has in recent years been a resurgence of interest in metal–matrix composites (MMC), arising at least in part from the current availability of several fibres with attractive features. Attention has in general been centred on the reinforcement of aluminium and its alloys, with the understanding that there are other candidates for future concerted study. The high performance potential of MMC systems (in terms of, for example, specific stiffness, tensile strength, wear resistance etc over a range of temperature) is well documented, but economic factors and, particularly, difficulties in developing viable fabrication routes have limited their commercial exploitation.

In this paper, data are presented on the use of a fibre recently developed specifically for MMC applications [1]. This is known as "Saffil"* alumina fibre, RF grade. It has a polycrystalline structure in which the predominant phase is δ-alumina. A few of the relevant properties of this fibre are compared in Table I with those typical of the main current alternatives, although some of the figures may conceal significant variations among individual fibres, both for a single product and between different commercial versions.

The fabrication and performance of MMCs based on these fibres in aluminium alloys is receiving intensive study [3–10]. In most cases there are problems in optimizing the wetting/bonding/distribution/damage characteristics during the fibre incorporation, although considerable progress is being made. The objective of the present paper is to outline some results from studies into the fabrication, structure and performance of composites containing the δ-alumina fibre.

The fibre is a rather fine one (≈ 3 μm diameter) and for the purposes of composite fabrication is chopped, milled and sized to give a preselected range of lengths. Typical distributions of diameter and length are shown in Fig. 1, giving in this case a fibre aspect ratio of around 100 to 200. For much of the composite fabrication, this material was further processed into pad-like preforms, incorporating a binder (see Section 2.2).

The δ-Al_2O_3 crystal structure is stabilized against transformation (at high temperature) to α-Al_2O_3 by the presence of about 3 to 4% SiO_2, which also tends to inhibit coarsening of the fine (50 nm) crystallite size. This silica is distributed throughout the δ-alumina phase and a thin

*"Saffil" is a trademark of Imperial Chemical Industries plc for its alumina fibres.

0022–2461/85 $03.00 + .12

TABLE I Selected fibre properties

Fibre	Mean diameter (μm)	Density (Mg m^{-3})	UTS (GPa)	E (GPa)	Reference
C	8	1.8	2.2	250	[2]
SiC	13	2.5	2	190	[3]
$K_2O(TiO_2)_6$ Cu-precipitated	0.2	3.3	$\geqslant 7$	280	[2]
$Li_2O.Al_2O_3.4SiO_2$	5	2.6	2	85	[4]
Al_2O_3/SiO_2	2.8	2.6	1.3	120	[2]
FP α-Al_2O_3	20	3.95	1.7	380	[5]
RF Saffil δ-Al_2O_3	3	3.3	2	300	[1]

(1–5 nm) silica-enriched layer forms on the free surface of the fibre. A δ–α transformation stimulates the appearance of the mullite phase ($3Al_2O_3 \cdot 2SiO_2$), which appears primarily at the grain boundaries: this tends to inhibit both further transformation and coarsening of the grain structure. A number of trace elements are present, but the total impurity content is typically < 0.2 wt% The material is effectively free from porosity Thermal stability is excellent up to around 1500 K Representative stiffness and room temperature tensile strength values were shown in Table I.

2. Composite fabrication

2.1. Fibre wetting and exploratory experiments

A number of studies [11–15] have confirmed that wetting is very poor between different forms of Al_2O_3 and molten aluminium, reported contact angles ranging from π near the melting point to $\geqslant \pi/3$ at 1800 K. Small changes in fibre or melt composition are unlikely to effect dramatic reductions in these values by a purely physical mechanism and most expedients aimed at improving the wetting have thus been designed to stimulate chemical reactions, often by way of fibre coatings or alloying additions. While artificial coating is cumbersome, alloying additions that can react chemically at the fibre/melt interface look attractive. For example, Al_2O_3 reacts with several divalent transition metal oxides to form alluminates isostructural with spinel ($MgO \cdot Al_2O_3$), offering the potential for the formation of strong interatomic bonds with both matrix and fibre. However, it would appear [6, 16–19] that only lithium (which forms $Li_2O \cdot 5Al_2O_3$) can rapidly

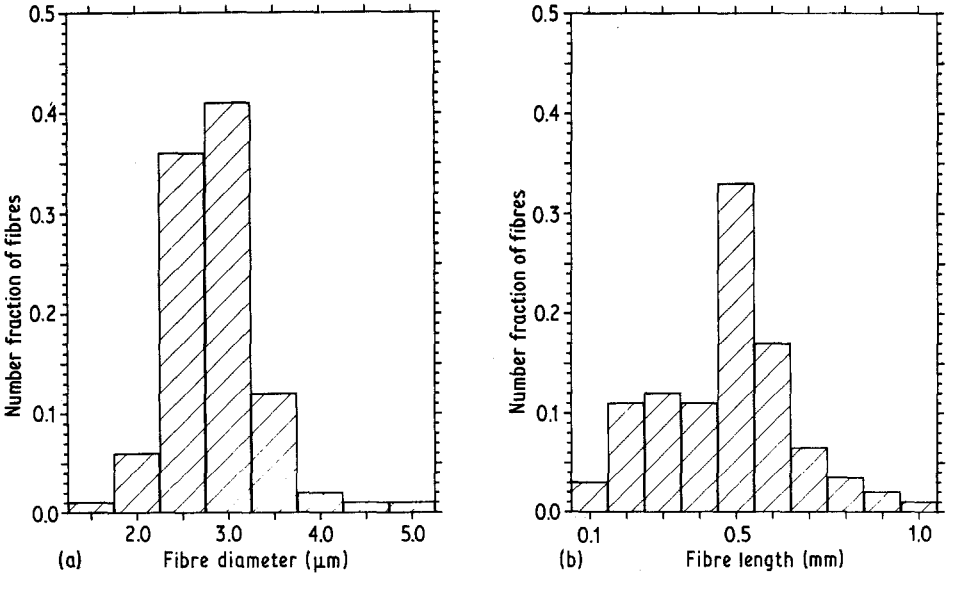

Figure 1 Distributions of (a) diameter and (b) length of δ-alumina fibres employed.

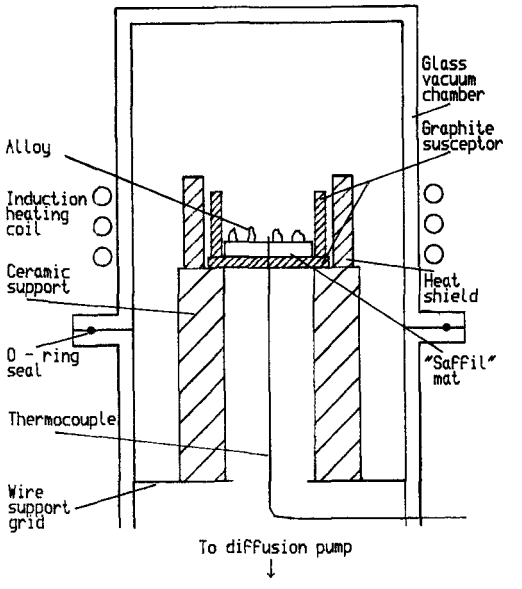

Figure 2 Schematic illustration of the rig designed for sorting of alloy droplets in terms of their propensity for wetting a fibre pad.

stimulate a suitable reaction (without requiring oxygen introduction, for example by agitation). Unfortunately, the incorporation of lithium can be associated with certain fabrication and handling problems.

A preliminary indication of the wetting behaviour of a range of alloys in contact with the fibre was obtained using the apparatus shown in Fig. 2. Small samples of up to 8 alloys were placed on a preformed pad of alumina fibres. The assembly was heated under vacuum, or controlled atmosphere, until the samples melted and their interaction with the pad was then observed. In no case was the droplet fully absorbed into the pad, but some wetting and penetration was observed. (This is a severe test since all aluminium alloys when heated in this way form a tenacious surface oxide film which inhibits pad/droplet contact.) Evidence of a degree of wetting was observed with some Al–Mg alloys and certain other systems exhibited marginal pad penetration. The test does not give a direct indication of the contact angle, because of the sensitivity to the oxide layer formation (which is influenced by the alloy composition). Nevertheless, and despite the limited scope of the tests, they provided a useful means of selecting the most promising alloy systems for subsequent work. Some hot-stage SEM studies were also helpful in this respect (see Section 3.2).

Initial fabrication attempts started with manual stirring of bulk and milled fibre into melts that were slowly cooling from initial superheats of up to about 300 K. The resultant mass was then decanted and manually tamped down into a warm (≈ 500 K) ingot mould. This produced porous but moderately compact and homogeneous ingots (with fibre volume fractions up to about 0.15 to 0.2) using Al–10 wt% Mg (LM10) and some other Al–Mg and Al–Si alloys: the operation was not successful with some melts, because of difficulties in wetting the fibres. These ingots were then densified by heating close to the nominal liquidus temperature and squeezing in a cylindrical die, using pressures of around 25 MPa. The resulting billets were generally sound (although containing some fine residual porosity and entrapped oxide).

While it proved to be possible, by using techniques such as the above sequence (and with methods involving premixing of fibres with metallic powder), to produce billets of reasonable quality, studies in these directions were superceded by the development of a melt infiltration technique offering an attractive combination of rapid processing and effective incorporation of fibres into the matrix.

2.2. Pressure-assisted network infiltration to form composites (PANIC)

2.2.1. Theory

Experimentation revealed that good composites could be produced by applying pressure to a fully liquid charge on the surface of a fibre pad located within a die. The apparatus is illustrated schematically in Fig. 3. Considerable interest is now being generated in the squeeze-infiltration of fibrous networks, and some studies have been recently reported: there are papers covering the squeezing of pre-mixed composites [6–9] and the pressurized infiltration of cylindrical SiC fibre bundles [3] and of a skeletal network of copper-precipitated devitroceramic fibre [2]. In addition, the patent literature contains guidelines [20–22] on conditions during pressurized pad infiltration. The process does not appear, however, to have been subjected to systematic process modelling analysis, although some recent Russian work has explored certain features [23, 24].

Resistance to penetration of the melt through the fibre network, which must be overcome by the applied pressure (perhaps assisted by capillarity), arises from at least two identifiable sources.

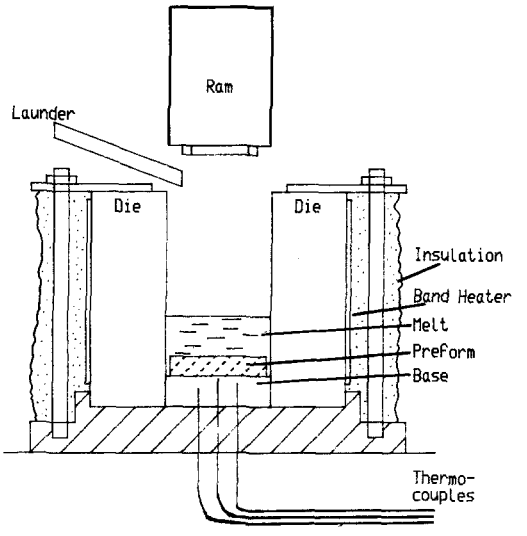

Figure 3 Schematic illustration of the set-up employed for pressure-assisted network infiltration to form composites (PANIC).

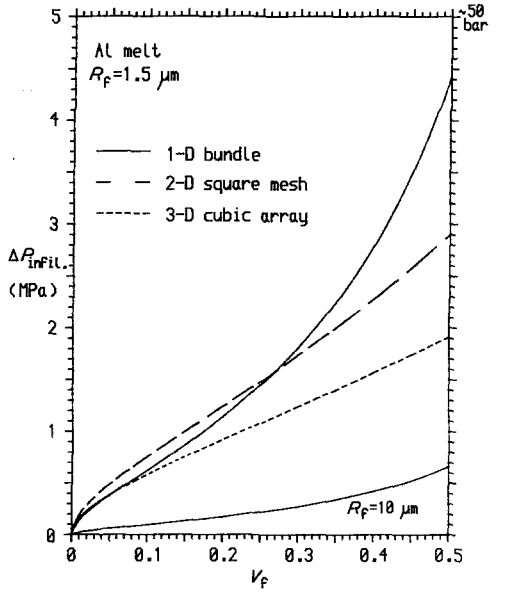

Figure 4 Predicted dependence of the pressure drop across the infiltration front on the volume fraction of fibre, for penetration of an aluminium melt into different types of fibrous array.

These are the effect of enforced meniscus curvature at the infiltration front and the resistance to flow (at a finite velocity) offered by the interstitial channels after passage of the front. The former is described by the familiar Kelvin equation

$$\Delta P = 2\gamma \sum_i \frac{1}{r_i}, \qquad (1)$$

where ΔP is the pressure drop across a surface exhibiting principal radii of curvature r_i, and γ is the interfacial energy. The curvatures imposed on the front depend on the volume fraction, V_f, radius, R_f, and distribution of the fibres: the assumption made about the degree to which fibre-melt wetting at the front reduces the curvatures is also important. If, as seems probable, wetting is insufficiently rapid (when the melt is penetrating relatively quickly) to allow curvature relaxation, and the minimum radius imposed corresponds to twice the inter-fibre spacing, the following expressions are obtained for different types of fibre array

$$\Delta P_1 = \frac{2\gamma}{R_f[(\pi/4V_f)^{1/2} - 1]} \qquad (2)$$

$$\Delta P_2 = \frac{4\gamma}{R_f[(\pi/2V_f)^{1/2} - 1]} \qquad (3)$$

$$\Delta P_3 = \frac{4\gamma}{R_f[(3\pi/4V_f)^{1/2} - 1]}, \qquad (4)$$

these relating to a one-dimensional bundle, two-dimensional square mesh and three-dimensional cubic array, respectively. Using the value [25] of 0.84 J m^{-2} for γ of aluminium, the behaviour predicted by these equations for fibres with the dimensions of "Saffil" is shown in Fig. 4. These curves suggest that the excess pressure to generate the curvature necessary for infiltration of even a fine, dense network is no greater than a few tens of atmospheres (or perhaps slightly more to ensure complete penetration into every fine crevice).

The second source of flow resistance is described by the Blake–Kozeny equation [26], which in the present case gives the following expression for the pressure gradient in the melt necessary to generate a flow velocity, u:

$$\frac{dP}{dZ} = 16.8\left[\frac{V_f}{R_f(1 - V_f)}\right]^2 u\eta, \qquad (5)$$

where η is the dynamic viscosity of the melt ($\approx 10^{-3}$ Pa sec for aluminium). This equation is valid only for laminar flow and the onset of turbulence [27] (expected for a packed-bed Reynolds number higher than 2) is predicted for pressure gradients greater than a critical value

$$\left(\frac{dP}{dZ}\right)_{crit.} = 67.2\left[\frac{V_f}{R_f(1 - V_f)}\right]^3 \frac{\eta^2}{\rho}. \qquad (6)$$

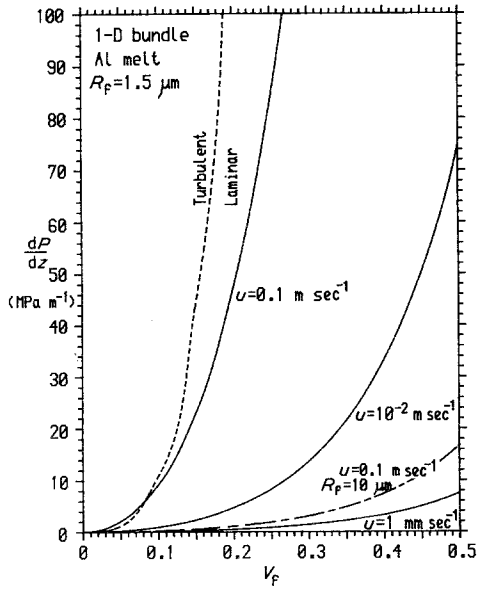

Figure 5 Predicted variation with volume fraction of fibre of the pressure gradient necessary to generate flow of an aluminium melt through a fibrous bundle at different velocities.

The pressure gradients necessary to generate flow at three different velocities are shown as a function of V_f for Saffil fibres in Fig. 5 (with a further curve for the 100 mm sec^{-1} case for a thicker fibre), together with the onset of turbulence boundary. This figure shows that (once the fibre network has been infiltrated) melt flow through the interstitial channels (to allow continued advance of the infiltration front) can occur at high velocities ($\simeq$ 10 mm sec^{-1}), even when the network is fine and dense, without requiring a pressure increment of more than about 10 atm (for infiltration depths of the order of a few tens of millimetres).

The Blake–Kozeny treatment refers to a steady state, whereas the actual infiltration is highly transient in several respects, but the curves shown should at least indicate what regime of penetration velocity is possible when a known external pressure is applied. It should be noted, of course, that the generation of a back-pressure in the gas ahead of the front (such as would arise if the melt flow were such as to isolate regions of the uninfiltrated pad from the air escape paths), would inhibit penetration and this can be of practical importance. In general, the overall process is a complex one, particularly when account is taken of pad compression and solidification behaviour. The incidence of fibre breakage, and local variations in V_f, in the final composite will be dependent on the degree of preform compression (itself related to local pressure gradients) and on the relative progress of the solidification fronts advancing from the ram and from the die base (after infiltration). Preliminary experimental and theoretical indications are that the contact time between the fibres and the quiescent melt is less than about a minute for the conditions used. Quantitative study of these aspects is currently being initiated.

2.2.2. Experimental findings

It has been found that fibre preforms of diameter 60 mm and up to about 40 mm thickness, containing fibre volume fractions in the approximate range 0.1 to 0.3, could be fully infiltrated by placing them in a die preheated to about 600 K and adding the alloy melt (superheated by about 100 to 200 K): this was followed by application of pressure in the range 25 to 75 MPa via a ram travelling at a nominal 9 mm sec^{-1}. Under suitable conditions, composites with very low levels of porosity and fibre damage can be produced from a range of melt compositions – including Al–Mg, Al–Si and Al–Cu alloys. Significant compression of the pad was noted under some conditions, and there were instances in which differential degrees of compaction were generated through the thickness of a single pad. An example of this is shown in Fig. 6.

The success of infiltration under these conditions is consistent with the theoretical predictions. It is clear from Fig. 4 that the pressure drop at the front is not expected to exceed a few MPa, while Fig. 5 suggests that the maximum infiltration velocity (which is limited in this case by the ram speed) requires pressure gradients ($\leqslant$ 25 MPa m^{-1}) which would easily be set up under the conditions employed. Turbulence within the infiltrating liquid appears impossible (at least with these fine fibres). Microstructural evidence suggests that the infiltration times are relatively short, although it has not yet been confirmed that they are as low as the minimum of a few seconds imposed by the ram speed. The major point remaining to be clarified in this respect concerns the possible inhibition of penetration by repeated oxide formation at the front.

2.3. Effect of preform characteristics

Although both predictions and experience have

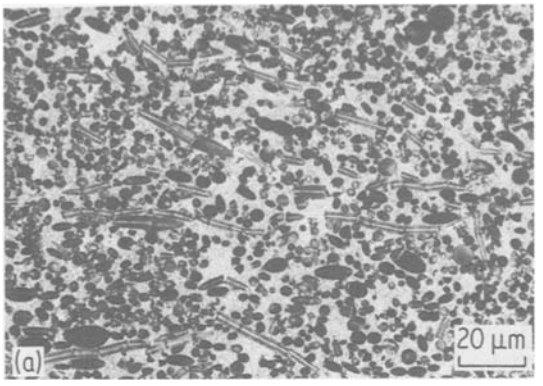

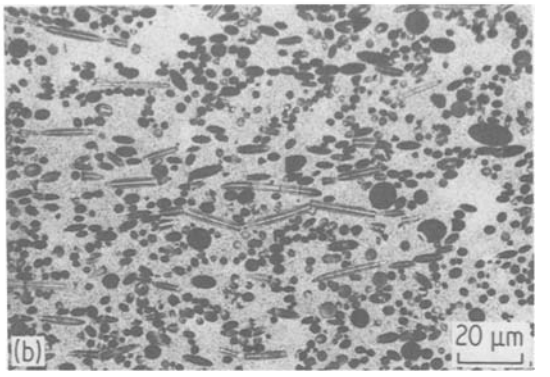

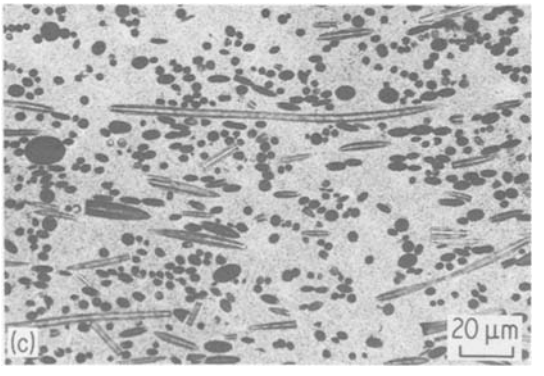

Figure 6 Optical micrographs of an LM10–18 vol% fibre composite: transverse sections taken at heights of approximately (a) 5 mm, (b) 10 mm, and (c) 15 mm above the die base.

suggested aluminium melt infiltration of a fine fibrous network to be possible under fairly modest applied pressures, the degree of wetting and thus the achievement of good fibre–matrix bonding in the resultant composite might be expected to exhibit some dependence on the system chemistry. In view of a suspected importance of the silica-rich surface layer, attempts were made to infiltrate preforms composed of fibres in which:

1. the normal silica binder level of 2.5 wt% had been reduced;
2. the silica binder had been replaced by a fugitive (latex) binding agent;
3. the silica-rich surface layer had been removed by etching with HF;
4. the δ-phase had been transformed to α-alumina by suitable heat treatments;
5. selected combinations of these treatments;

and attempts were made to infiltrate these with LM6 (Al–12 wt% Si) alloy under a standardized set of conditions, the resultant composites then being examined by optical metallography.

The level of silica binder was found to have no influence on the infiltration behaviour, although low values (< 1.0%) result in poor handling strength and very high levels (> 15%) are expected to start to inhibit flow of the melt. Preforms made with the fugitive binder were very weak and friable after the latex had been driven off, but they could still be successfully infiltrated. This was also true of preforms containing no silica (either in the binder or on the fibre surface), although there was, in this case, a very slight suggestion of a little residual porosity in a few inter-fibre crevices. Fibres that had been converted to the α form were also fully infiltrated, although in this case their appearance was slightly altered (as a result of the phase transformation and attendant changes, such as a large increase in grain size).

The success of the physical penetration and envelopment of the fibrous array would thus appear to be dependent solely on the physics of the process (including the setting up of a suitable thermal field), which is consistent with the basis of the analysis in Section 2.2.1. The strength of the fibre–matrix bond cannot, however, be inferred reliably from visual examination and investigations of the effect of the fibre chemistry in this regard are proceeding.

3. Microstructural features

3.1. Fibre distribution

Little relative fibre motion occurs during the PANIC process and the distribution in the composites was essentially that inherited from the pad (normally a random planar array). This was, for example, indicated by optical micrographs such as those of Fig. 6, in which the fibre texture may be deduced by examining the elliptical fibre cross-sections in terms of the eccentricity and

TABLE II Fibre length data before and after incorporation in an Al–9% Si–3% Cu matrix

Volume fraction of fibre in pad	Mean fibre length (μm)		Fraction < 120 μm	
	Initial	Extracted	Initial	Extracted
0.12	228	180	0.17	0.28
0.18	182	162	0.24	0.30
0.24	172	156	0.30	0.38

orientation distributions of the major axes. Some evidence is apparent of a certain degree of fibre breakage, although the limited nature of this damage under typical conditions was confirmed by the fibre length measurements shown in Table II, which compares values from the initial pad with those obtained after extraction from the composite. It was also noted from micrographs such as those of Fig. 7 that the grain structure within the infiltrated pad was much finer than elsewhere and that grain boundaries were linked to fibres. This may be partly a result of many of them having acted as effective substrates for nucleation of matrix crystals, which is not surprising in view of the apparently excellent wetting under the conditions of infiltration.

3.2. Interface structure

Definitive examination of the fibre–matrix interface region was hindered by the scale of the structure, which is, for example, small relative to the X-ray emission volume excited by an electron beam at normal accelerating voltages. However, it was possible, by using X-ray photoelectron spectroscopy (XPS) on virgin and extracted fibres, to investigate chemical changes at the fibre surface. For example, Fig. 8 compares spectra for (a) untreated fibres with (b) fibres extracted from a composite formed with LM10, by dissolution with 10% iodine in methanol.

These data should be interpreted with care. The Si_{2s} peak at about 150 eV (representing about 3 to 4 at % Si) is largely unchanged in magnitude (as is the Si/Al ratio) and shows that silicon is present as SiO_2; there is no evidence of a peak corresponding to elemental (zero valence) silicon, which would have been expected at an easily detectable shift of about 4 eV below the Si_{2s}. This suggests that the SiO_2 in the surface layers had not been chemically reduced: it should be noted, however, that the fibre extraction was not carried out under anaerobic conditions, so that any elemental silicon that did form would have been subsequently reoxidized, although probably to a depth of only about 1 nm or so (as compared to the escape depth for this photoelectron of about 5 nm). The implication is thus that any reduction of the silica in the fibre surface cannot have penetrated beyond a few atomic layers. It also follows that, if such a surface attack did take place, the reaction products could not have been subsequently swept away (suggesting that the melt must have been quiescent at the time).

However, the appearance of the Mg^{2+} peaks in the second spectrum is also significant. These are of three types, corresponding to the 1s photoelectrons (at 1305 eV), the Auger *KLL* electrons (at 300 to 400 eV) and the 2p and 2s photoelectrons (at 52 and 89 eV), these having escape depths of about 2, 4 and 5 nm, respectively [28, 29]. The magnitudes of these peaks are relatively high in all three categories (and are, in fact, of the same order as would be expected for the spinel structure), implying that the Mg^{2+} ion is present at appreciable concentrations to depths of at least several atomic layers. The occurrence

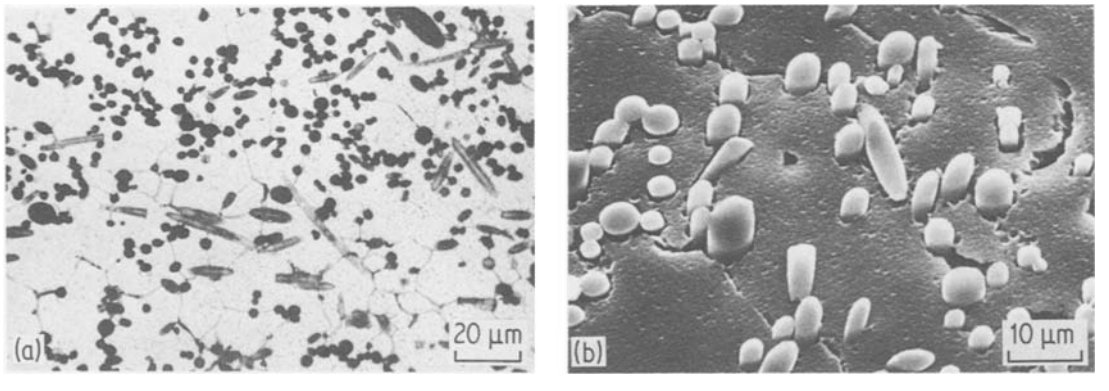

Figure 7 (a) Optical and (b) SEM micrographs of an LM10–18 vol% fibre composite, showing the grain structure.

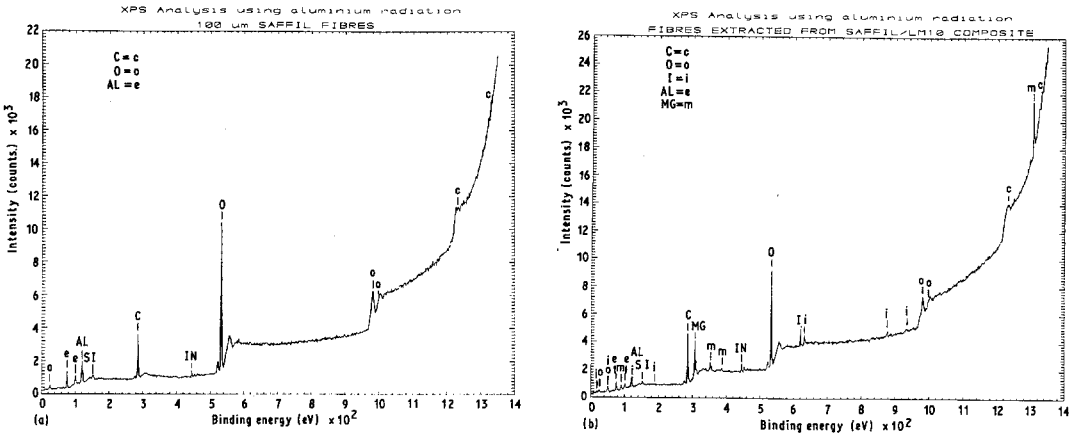

Figure 8 XPS spectra from (a) virgin Saffil fibres and (b) fibres extracted from composite with LM10.

of Mg^{2+} peaks of all three types strongly suggests that the magnesium was not simply deposited as a hydroxide precipitated as the matrix dissolved during extraction (as might have been feared [30]), but rather that the Mg^{2+} ion is present in the lattice throughout the surface layers of the fibre. (If all three types of peak had been due to excitation from a thick deposited $Mg(OH)_2$ layer, then the silicon and aluminium signals would have been lower than those from the virgin fibre.) In summary, a chemical reaction has occurred in which a melt constituent enters the surface layers of the fibre, but if this process involves any reduction in the oxidation state of silicon within these layers, then it must be a highly surface-specific effect.

The high strength of the interfacial bond was evident in several ways. For example, a typical fracture surface after tensile testing (see Section 4.1), such as that of Fig. 9, showed no evidence of fibre pull-out. Hot-stage SEM work also indicated a high melt-fibre affinity: for example, imaging of partially unwetted fibres (from specimens for which infiltration had been deliberately limited) indicated a tendency for the matrix, once molten, to move along the fibre (Fig. 10), although this was inhibited by the presence of the oxide film.

A further important feature of the behaviour of the system at elevated temperature concerns the high thermal stability of the fabricated composite. Certainly, no apparent degradation of the structure took place even under protracted conventional heat treatments. In fact, holding the composite at temperatures corresponding to a semisolid or fully liquid matrix, while it clearly tends to produce some changes in the appearance of the matrix (depending in part on how the subsequent solidification is carried out), did not lead to impaired integrity of the fibre array. The structure shown in Fig. 11 is that of a composite held for 2 days at 900° C and then slowly cooled.

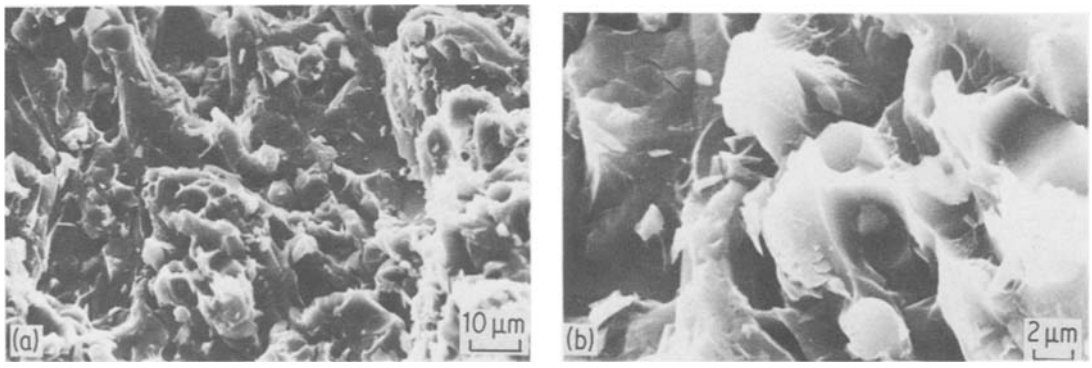

Figure 9 SEM micrographs at two magnifications of a fracture surface produced by tensile testing of an LM6–18 vol% composite, showing the virtual absence of any fibre "pull-out" or interfacial delamination.

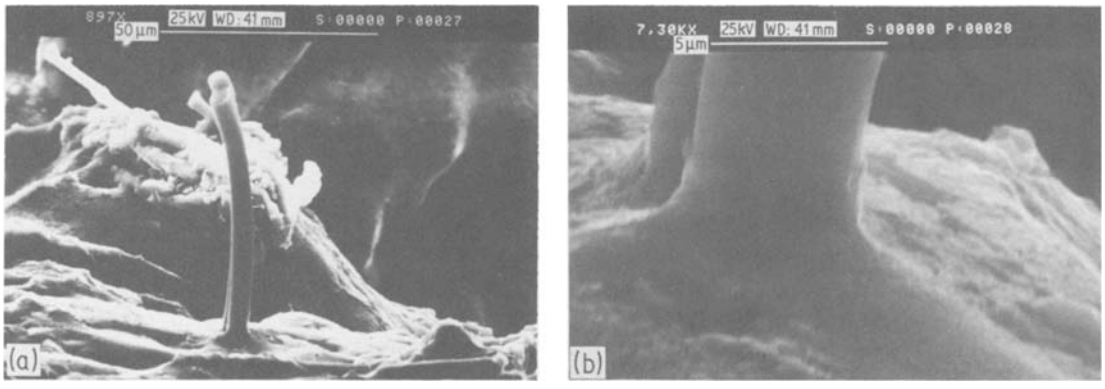

Figure 10 Hot-stage SEM micrographs showing the root area of an initially unwetted fibre.

Although there is some evidence of attack in this case, the thermal stability under more conventional conditions is clearly expected to be exceptionally high. The stability of these melt–fibre mixtures at sustained high temperatures may be affected by any phase transformation taking place in the alumina, although in this case the δ-phase would probably have remained stable [31].

3.3. Matrix structure

In agreement with previous observations [32], the structure of the matrix phase in the composites was found to be different from that in unreinforced material solidified under similar conditions. There is a reduction in grain size (by a factor of perhaps 100 to around 20 to 40 μm mean diameter) – see Fig. 8. Microhardness tests were carried out in the matrix material on both the fibre-reinforced and fibre-free regions of infiltrated billets. The results are presented in Table III. This shows a significant increase in hardness in the fibre-reinforced region, which may be attributed to changes in the matrix structure [32] and constraint from the array of fibres nearby.

There is, in addition to these changes to the aluminium solid solution structure, a marked tendency for the appearance of any second phase to be strongly affected by the presence of the fibres. This is illustrated by Fig. 12, consisting of two micrographs from a composite produced with an Al–Si eutectic alloy. It is clear from the micrograph at lower magnification, which shows an area near the top of the preform, that the eutectic growth mode has been severely disturbed by the presence of the fibres. This is an unmodified alloy, but the high cooling rate would normally give rise [33] to the fine fibrous eutectic structure apparent in the upper portion of this micrograph. The coupling at the eutectic growth front has clearly been disturbed by the presence of the fibres and it seems very unlikely that this

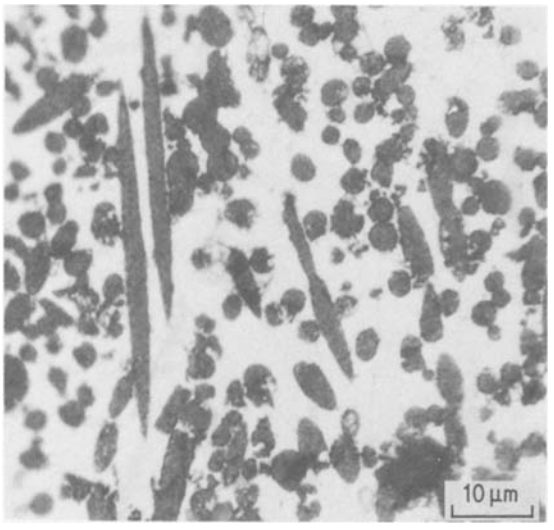

Figure 11 Optical micrograph of an LM10–18 vol% fibre composite after holding for 2 days at 900° C.

TABLE III Microhardness data from fibre-free and reinforced matrices of some aluminium alloys

Alloy	Fibre volume fraction	Mean microhardness (kg mm^{-2})	
		Inter-fibre matrix	Fibre-free matrix
Al–10 Mg	0.18	105	95
Al–10 Mg	0.30	115	94
Al–10 Mg	0.40	118	90
Al–11.5 Si	0.24	96	72
Al–4 Cu	0.24	115	77

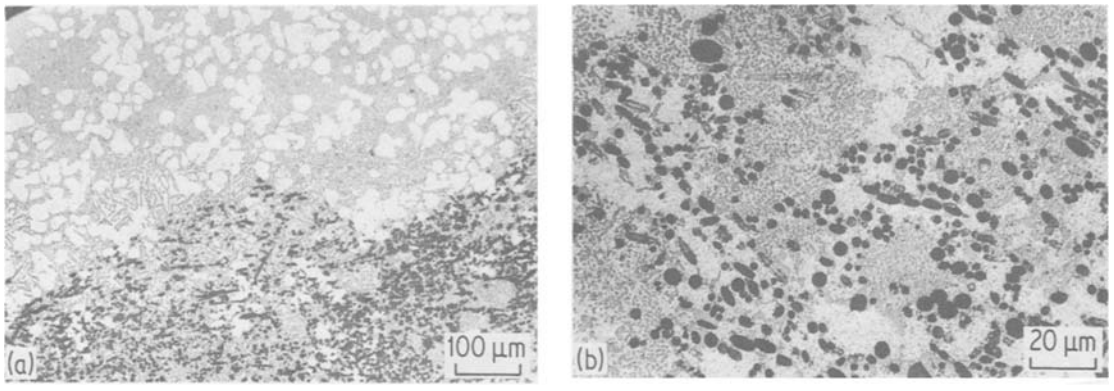

Figure 12 Optical micrographs of an LM6–18 vol% fibre composite, showing the change in microstructure between the fibre-free and infiltrated areas.

could be due to any reduction in the cooling rate in this region.

Inspection of the second micrograph reveals that the effect appears to be associated with preferential nucleation of the silicon phase on the fibre surfaces. This appears not only to have disturbed the eutectic growth (producing a coarse and partially divorced [34] structure), but also to have reduced somewhat the incidence of primary aluminium (which is often appreciable, even in a nominally eutectic composition, at high cooling rates [33]). It may be noted that changes of this type may have unfavourable effects on the mechanical properties, such as an expected increase in brittleness for the example shown. This highlights the importance of tailoring the alloy composition to the fabrication and performance requirements of these composites. It would appear, for example, that the high melt fluidity for which alloys such as LM6 are traditionally favoured is not a prerequisite for successful infiltration and the avoidance of embrittling constituents should probably be given a high priority in formation of these composites. Certainly, test pieces produced from the specimen shown were very prone to low ductility problems.

4. Mechanical properties

A number of flexural and tensile test pieces have been taken from billets made with the PANIC rig. Insufficient testing has been completed to fully characterize the materials, but Young's modulus measurements around 100 GPa and tensile strengths of 280 MPa have been recorded. A more extensive programme of testing has been undertaken on composites, based on a commercial Al–9% Si–3% Cu alloy, produced under similar conditions using industrial equipment. Tensile test data are shown in Table IV and Fig. 13.

It will be noted that the tensile modulus at room temperature ranges from 100 to 114 GPa for these fibre volume fractions. These increases (over a value of about 70 GPa for the unreinforced alloy) are close to the maximum expected with a random planar array [35] of fibres, implying both that the fibre–matrix bonding is strong and that the fibre aspect ratio is sufficiently high for a uniform tensile load to be borne over much of their length. The strength at 25° C is not improved significantly when compared with an unreinforced pressure casting of this alloy, but at elevated temperatures the higher V_f materials are markedly stronger. Both strength and modulus fall as the temperature is raised; however, the modulus at 300° C with only 12% fibre is no lower than that of an unreinforced matrix at room temperature and the strength retention at 300° C (and above) of all the composites represents a major improvement on the of conventional cast aluminium alloys. It should be noted, however, that the strength increases are accompanied, as expected, by marked reductions in ductility, although some evidence of significant plastic deformation starts to appear in the stress–strain curves for the higher testing temperatures. The low ductility and consequent susceptibility to the effect of stress-raisers, is probably responsible for the failure to realize the full strengthening potential at room temperature: this suggests that the use of matrix material with a very high ductility could result in improvements to certain properties.

TABLE IV Tensile properties of composites made by preform infiltration with Al–9% Si–3% Cu

Fibre fraction	Test temperature (° C)	Young's modulus (GPa)	Tensile strength (MPa)	Strain to fracture (%)
0.12	25	100	318	0.6
	100	90	268	0.8
	200	79	229	0.7
	250	73	188	0.9
	300	67	154	1.2
0.18	25	107	312	0.5
	100	103	304	0.5
	200	90	240	0.8
	250	84	215	0.8
	300	77	182	0.8
0.24	25	114	213	0.4
	100	115	292	0.4
	200	105	282	0.7
	250	93	244	0.6
	300	86	196	0.7
Typical as-cast Al–9% Si–3% Cu	300	–	50–100	6.0

5. Discussion and conclusions

A technique has been presented for the fabrication of MMC billets, involving the pressurized infiltration of a fibrous preform pad with a superheated melt. It has been found that, with a suitable combination of the operating variables and employing a fine δ-alumina fibre recently made available for MMC applications, composites based on a range of aluminium alloys can be fabricated in this way. A high degree of control is retained over the fibre orientation and distribution, which are essentially as inherited from the preform. The levels of porosity and fibre damage are very low and all the evidence points to a very strong matrix–fibre interfacial bonding. Some of the characteristics of the fabrication process have been explored in a preliminary manner, particularly with respect to the pressure and infiltration rate characteristics. These treatments have shown that only relatively modest pressures should be necessary to ensure quite rapid penetration of the fibre network concerned, and this has been borne out by the experimental information available to date.

However, it is possible that good fibre–matrix bonding is dependent, not only on the setting up of suitable pressure and temperature fields during the infiltration, but also on the system chemistry. The presence of magnesium in the melt seems to promote particularly strong wetting, although good structures have been produced with a wide range of other alloys. The evidence presented suggests that the thin, silica-rich layer on the fibre surface does not take part in a chemical reaction during infiltration and the subsequent melt contact period (which has been rather short in the current work), unless such a reaction extends to a depth of no more than a very few atomic layers. It is clear, moreover, that after formation of the

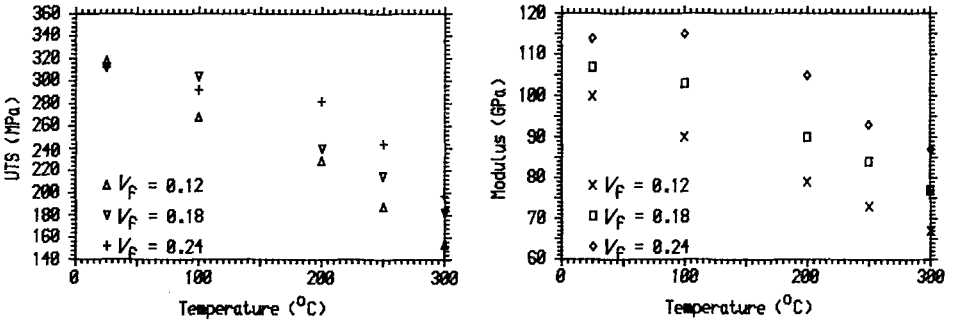

Figure 13 Tensile strength and modulus of Al–9% Si–3% Cu-based composites, showing the variation with testing temperature.

composite, the fibres remain very stable on heating and, indeed, on remelting, of the matrix, even under extended treatment at elevated temperatures.

A fairly comprehensive series of mechanical tests have been applied to MMCs fabricated in this way, covering a range of testing temperatures. The levels recorded for both stiffness and strength confirmed the microstructural impression that fibre integrity was unimpaired during fabrication and that matrix–fibre bonding was very strong. The enhancement in strength when compared with an unreinforced as-cast alloy is substantial at elevated temperatures. It might prove profitable to explore the development of alloys specifically designed for MMC applications.

Acknowledgements

The authors would like to acknowledge the financial support provided by ICI Mond Division under a Joint Research Scheme with the University of Surrey. Particular appreciation is expressed to Mr J. Dinwoodie, of ICI Mond, and to Professor J. D. Birchall, of the ICI New Science Group, who have been of considerable scientific and technical assistance in this work. Thanks are also due to Dr J. F. Watts, of the Surface Analysis Laboratory in the University of Surrey, for his informative collaboration and advice.

References

1. Data sheet on RF Saffil, ICI Mond division, Runcorn, Cheshire, UK (1982).
2. T. DONOMOTO, K. FUNATANI, N. MIURA and N. MIYAKE, "Ceramic Fibre Reinforced Piston for High Performance Diesel Engines", paper 830252, SAE Int. Congress and Exposition, Detroit, 28 February to 4 March (1983).
3. H. FUKUNAGA and M. KURIYAMA, *Bull. JSME* **25** (1982) 842.
4. H. FUKUNAGA, "Rotating Bending Fatigue Strength of Copper-precipitated Devitroceramic Fibre Reinforced Aluminium", 24th Japanese Congress on Materials Research on Metallic Materials, March (1981) pp. 130–3.
5. C. G. LEVI, G. J. ABBASCHIAN and R. MEHRABIAN, *Met. Trans.* **9A** (1978) 697.
6. F. M. HOSKING, F. FOLGAR PORTILLO, R. WUNDERLIN and R. MEHRABIAN, *J. Mater. Sci.* **17** (1982) 477.
7. K. J. BHANSALI and R. MEHRABIAN, *J. Metals* **34**(9) (1982) 30.
8. D. WEBSTER, *Met. Trans.* **13A** (1982) 1511.
9. B. F. QUIGLEY, G. J. ABBASCHIAN, R. WUNDERLIN and R. MEHRABIAN, *ibid.* **13A** (1982) 93.
10. G. H. PIGOTT and J. ISHMAEL, "A Strategy for the Design and Evaluation of a Safe Inorganic Fibre", 5th International Symposium on Inhaled Particles, Cardiff, September (1980).
11. K. PRABRIPUTALOONG and M. R. PIGGOTT, *Surf. Sci.* **44** (1974) 585.
12. S. M. WOLF, A. P. LEVITT and J. BROWN, *Chem. Eng. Prog.* **62** (1966) 74.
13. J. BRENNAN and J. A. PASK, *J. Amer. Ceram. Soc.* **51** (1968) 569.
14. S. K. RHEE, *ibid.* **55** (1972) 300.
15. W. KOHLER, *Aluminium* **7** (1975) 443.
16. R. MEHRABIAN, "A Fundamental Study of a New Fabrication Technique for Fiber Reinforced Aluminium Matrix Composites", Final Report on US Army Research Office Contract DAAG29-76-G-0170, April (1980).
17. S. V. PEPPER, *J. Appl. Phys.* **47** (1976) 801.
18. A. MUNITZ, M. METZGER and R. MEHRABIAN, *Met. Trans.* **10A** (1979) 1491.
19. A. K. DHINGRA and W. H. KREUGER, "Fiber FP Continuous Yarn", Report by E. I. DuPont de Nemours & Co. Inc., Wilmington, DL (1974).
20. UK Patent No. 1 567 328, May (1980).
21. R. W. GRIMSHAW and C. POOLE, UK Patent No. 1 595 280, August (1981).
22. K. BAN, A. DAIMARA, Y. MURAOKA and N. MIYAKE, UK Patent No. 2 088 761, June (1982).
23. K. I. PORTNOI, S. E. SALIBEKOV, I. L. SWETLOV and V. M. CHUBAROV, "Structure and Properties of Composite Materials" (Mashinostroenie, Moscow, 1979) in Russian.
24. S. T. MILEIKO, in "Fabrication of Composites", edited by A. Kelly and S. T. Mileiko (North Holland, Amsterdam, 1983) p. 287.
25. J. SZEKELY, "Fluid Flow Phenomena in Metals Processing" (Academic Press, New York, 1979) p. 237.
26. S. ERGUN, *Chem. Eng. Prog.* **48** (1952) 93.
27. G. H. GEIGER and D. R. POIRIER, "Transport Phenomena in Metallurgy" (Addison-Wesley, New York, 1973) p. 94.
28. M. P. SEAH and W. A. DENCH, *Surf. Interface Anal.* **1** (1979) 2.
29. J. F. WATTS and J. E. CASTLE, *J. Mater. Sci.* **18** (1983) 2987.
30. W. H. J. VERNON, F. WORMWELL and T. J. NURSE, *J. Chem. Soc.* (1939) 621.
31. W. R. SYMES and E. RASTETTER, in 24th International Colloquium on Refractories, Aachen, September 1981.
32. R. J. ARSENAULT and R. M. FISHER, *Scripta Metall.* **17** (1983) 67.
33. R. ELLIOTT, *Int. Met. Rev.* **22** (1977) 161.
34. W. KURZ and D. J. FISHER, *Int. Met. Rev.* **24** (1979) 177.
35. R. M. CHRISTENSEN and R. M. WAALS, *J. Comp. Mater.* **6** (1972) 518.

Received 23 February
and accepted 9 March 1984